THE JOURNAL OF BIOLOGICAL CHEMISTRY VOL. 284, NO. 52, pp. 36248–36261, December 25, 2009

Regulation of TRPC1 and TRPC4 Cation Channels Requires an α1-Syntrophin-dependent Complex in Skeletal Mouse Myotubes*[S]

Received for publication, April 24, 2009, and in revised form, September 25, 2009 Published, JBC Papers in Press, October 7, 2009, DOI 10.1074/jbc.M109.012872

Jessica Sabourin, Coralie Lamiche, Aurelie Vandebrouck, Christophe Magaud, Jerome Rivet, Christian Cognard, Nicolas Bourmeyster, and Bruno Constantin[1]

From the Institut de Physiologie et Biologie Cellulaires, UMR CNRS 6187, Université de Poitiers, 86022 Poitiers, France

The dystrophin-associated protein complex (DAPC) is essential for skeletal muscle, and the lack of dystrophin in Duchenne muscular dystrophy results in a reduction of DAPC components such as syntrophins and in fiber necrosis. By anchoring various molecules, the syntrophins may confer a role in cell signaling to the DAPC. Calcium disorders and abnormally elevated cation influx in dystrophic muscle cells have suggested that the DAPC regulates some sarcolemmal cationic channels. We demonstrated previously that mini-dystrophin and α1-syntrophin restore normal cation entry in dystrophin-deficient myotubes and that sarcolemmal TRPC1 channels associate with dystrophin and the bound PDZ domain of α1-syntrophin. This study shows that small interfering RNA (siRNA) silencing of α1-syntrophin dysregulated cation influx in myotubes. Moreover, deletion of the PDZ-containing domain prevented restoration of normal cation entry by α1-syntrophin transfection in dystrophin-deficient myotubes. TRPC1 and TRPC4 channels are expressed at the sarcolemma of muscle cells; forced expression or siRNA silencing showed that cation influx regulated by α1-syntrophin is supported by TRPC1 and TRPC4. A molecular association was found between TRPC1 and TRPC4 channels and the α1-syntrophin-dystrophin complex. TRPC1 and TRPC4 channels may form sarcolemmal channels anchored to the DAPC, and α1-syntrophin is necessary to maintain the normal regulation of TRPC-supported cation entry in skeletal muscle. Cation channels with DAPC form a signaling complex that modulates cation entry and may be crucial for normal calcium homeostasis in skeletal muscles.

Dystrophin is a large cytoplasmic protein located at the inner face of the sarcolemma in muscle cells. The N-terminal portion of the protein binds actin, and the C-terminal portion binds β-dystroglycan, which is part of the dystrophin-glycoprotein complex; this complex is believed to provide a framework that connects the extracellular matrix to the intracellular cytoskeleton (1). Because of this structural organization, dystrophin has been postulated to protect fibers against mechanical damage. Knowledge of the role of dystrophin in skeletal muscle has been gained by intensive studies of muscles from patients suffering from Duchenne muscular dystrophy (DMD)[2] as well as from *mdx* mice, the animal model of the genetic disease. In very severe DMD phenotypes, the total absence of dystrophin leads to necrosis of skeletal muscle and results in a reduction or complete absence of dystrophin-associated protein complex (DAPC) components such as sarcoglycans and syntrophins (2, 3).

The syntrophins are a family of intracellular peripheral membrane proteins. The binding of syntrophins to a variety of channels or enzymes has contributed to the idea that these proteins are molecular adaptors that confer a signaling role to the DAPC. α1-Syntrophin is the predominant syntrophin isoform in skeletal and cardiac muscles (4). This adaptor protein binds transmembrane channels, such as sodium channels SkM1 and SkM2 (5) or the potassium channel Kir4.1 (6), through a PDZ (PSD95-disc large-zona occludens) domain.

In skeletal muscle, we have demonstrated for the first time that endogenous TRPC1 channels form a macromolecular complex with the costameric proteins α1-syntrophin and dystrophin and bind to the PDZ domain of the α1-syntrophin (7). TRPC1 has been shown to interact with other scaffolding proteins such as Homer (8) and caveolin-1 (9).

The TRPC1 protein is one element of certain non-voltage-gated heteromeric cation channels involved in Ca^{2+} and Na^{+} pathway, which can be activated in response to agonist-stimulated phosphatidylinositol 4,5-bisphosphate hydrolysis; it is thought to be a component of store-operated channels (SOCs) in various tissues (10). Recently, the study of salivary gland cells from $TRPC1^{-/-}$ mice showed that TRPC1 is necessary for store-operated currents in this tissue (11), whereas the analysis of platelets from $TRPC1^{-/-}$ mice showed that store-operated calcium entry (SOCE) occurs independently of TRPC1 (12). Two other proteins, STIM1, a single transmembrane protein (stromal interaction protein 1) and Orai1, a four-transmem-

* This work was supported by the CNRS, the French Ministry of Research, and the Association Française contre les Myopathies.

[S] The on-line version of this article (available at http://www.jbc.org) contains supplemental Figs. S1 and S2 and Table 1.

[1] To whom correspondence should be addressed: Institut de Physiologie et Biologie Cellulaires, UMR CNRS 6187, Université de Poitiers, 86022 Poitiers Cedex, France. E-mail: bruno.constantin@univ-poitiers.fr.

[2] The abbreviations used are: DMD, Duchenne muscular dystrophy; DAPC, dystrophin-associated protein complex; SOC, store-operated channel; SOCE, store-operated calcium entry; MS, mechanosensitive; siRNA, small interfering RNA; shRNA, short hairpin RNA; FL, full-length; GFP, green fluorescent protein; EGFP, enhanced green fluorescent protein; GST, glutathione *S*-transferase; BSA, bovine serum albumin; TRITC, tetramethylrhodamine isothiocyanate; FAM, 6-carboxyfluorescein; TAMRA, 6-carboxytetramethylrhodamine; SERCA, sarcoplasmic/endoplasmic reticulum Ca^{2+} ATPase.

brane domain protein, have emerged as components of the store-operated channels (13, 14) and can interact with TRPC proteins in a heteromeric complex to confer responsiveness to store depletion in various cells (15–17). In muscle fibers, the study by Kurebayashi and Ogawa in 2001 (18) showed that complete or partial depletion of sarcoplasmic reticulum stores during repetitive activation of calcium release stimulates store-operated calcium entry. Recent studies have revealed high levels of Orai1 (19) and STIM1 at the membrane of the sarcoplasmic reticulum (20) in skeletal muscle as well as a requirement for STIM1 in SOCE and in the contractile function of skeletal muscle (20). The localization of STIM1 at the sarcoplasmic reticulum suggests its involvement in the activation of SOCs and calcium influx through the membrane of T-tubule, which occurs after calcium release (21).

At the sarcolemma, TRPC1 and TRPC4 are involved in a cationic channel with activity enhanced by the depletion of calcium stores by thapsigargin (22) and with many biophysical properties similar to those of the mechanosensitive (MS) channels recorded in the same preparation (23). Moreover, a stretch-activated channel, as well as a SOC, was shown to be encoded by the TRPC1 gene (24). Taken together, these data suggest that MS channels and SOCs may represent the same channel, constituted by at least TRPC1. The activity of MS channels (25–27) and SOCs (22) is higher in dystrophin-deficient muscle cells. The sarcolemma of dystrophin-deficient muscle also displays cation channels that are active when muscles are at rest, with greater open probability (28), and an antisense strategy suggested that the spontaneously active channels are constituted by TRPC protein (22). These studies and others led to the hypothesis that the DAPC may control TRPC-MS/SOC channels at the sarcolemma and that is involved in regulating subsarcolemmal calcium concentration. These channels could be regulated directly in normal cells by the presence of the DAPC, which could explain the enhanced SOCE observed in dystrophin-deficient muscles (29, 30). In accordance with this idea, we recently reported that when transfected in dystrophin-deficient myotubes, recombinant mini-dystrophin or α1-syntrophin forms a complex with TRPC1 channels and restores normal divalent cation entry after store depletion (7). Because TRPC1 has the ability to form heteromeric channels, the association with other TRPC was explored. Several contributions have shown that TRPC1 and TRPC4 associate to build a cation channel that is permeable to calcium (31) and that reducing TRPC1 and TRPC4 expression decreases the occurrence of store-operated currents recorded at the sarcolemma of muscle fibers (22).

These data and the association of TRPC1 with endogenous complex α1-syntrophin/dystrophin prompted us to investigate whether α1-syntrophin, the predominant syntrophin isoform in striated muscle, could play a crucial role in regulating the sarcolemmal cation channels supported by TRPC1 and TRPC4. We thus performed small interfering RNA (siRNA) experiments to establish whether the reduction of α1-syntrophin could result in cation influx deregulation. Deletion of the N terminus corresponding to the PH1a (pleckstrin homology 1a) and PDZ domains, as well as forced expression of the deleted α1-syntrophin in dystrophin-deficient myotubes, was also performed to determine whether the N-terminal domain is necessary for this regulation.

EXPERIMENTAL PROCEDURES

cDNA Constructs and Recombinant Proteins

Full-length (FL) *Mus musculus* α1-syntrophin cDNA was obtained from Stephen Gee (University of Ottawa, Canada) and subcloned in pCMS-enhanced GFP with NheI and NotI restriction enzymes and with two tandem N-terminal Myc epitope tags. The ΔN-α1-syntrophin was obtained by deleting a 162-bp fragment, which corresponds to the PH1a and PDZ domains. This cDNA was ligated into bicistronic pCMS-enhanced GFP. The GST-PDZ domain (amino acids 75–170 of α1-syntrophin) was obtained and produced by means of the plasmid pGEX-5X-3. Recombinant proteins were prepared as GST fusion proteins in *Escherichia coli* (Tg1), purified using glutathione-Sepharose beads (Amersham Biosciences), eluted with glutathione, and used as GST fusion proteins. Plasmids containing the cDNA of TRPC1 and TRPC4 were obtained from Dr. Craig Montell (The Johns Hopkins University School of Medicine, Baltimore).

Cell Culture and Transfections

Experiments were performed on two cell lines: dystrophin-deficient dys$^-$ SolC1 and one expressing mini-dystrophin minidys+ SolD6. These cell lines were cultured as described elsewhere (30). Transfection was performed on proliferative myoblasts, and experiments were performed on myotubes at days 3 and 4 after initiation of myoblasts fusion. For primary cultures, the procedure was as described elsewhere (7). Myoblasts were transfected on the day of seeding in plastic dishes or glass coverslips using Nucleofector transfection (Amaxa Biosystems, Cologne, Germany). One million cells were centrifuged at 90 × *g* at room temperature for 10 min and resuspended at room temperature in Nucleofector solution (Nucleofector kit V) to a final concentration of 1 million cells/100 μl. The 100-μl cell suspension was mixed with plasmid solution prepared with a Qiagen plasmid purification maxi kit (Qiagen, Courtaboeuf, France). For single transfection of syntrophin in bicistronic plasmid, 2 μg of ΔN-α1-syntrophin-EGFP or FL-α1-syntrophin-EGFP was diluted in cell suspension. For double transfection of TRPC1 or TRPC4 with EGFP, the 100-μl cell suspension was mixed with 1 μg of pmaxGFP and 5 μg of TRPC1 or TRPC4 plasmids. The cell suspension was submitted to a pulse protocol (Amaxa B-032, kit V) for nucleotransfection (Amaxa Biosystems). 500 μl of prewarmed culture medium was added to transfected cells, and the mix was added to the myoblasts.

Silencing of α1-Syntrophin, TRPC1, and TRPC4 Expression

We obtained mouse SolD6 myotubes with reduced α1-syntrophin expression using transient transfection of siRNA. The siRNA silencing sequence (5′-AAGGUAUGAAUGUGCCGAUCUGCGC-3′ (Eurogentec, Seraing, Belgium)) was designed to target mouse α1-syntrophin mRNA (GenBank™ accession number NM_009228). SiRNA and its control (sequence with no homology with any known eukaryotic gene; Eurogentec) were

transfected at 3 μg/1 million cells into SolD6 myoblasts using a Nucleofector transfection device. Silencing was also performed using the same transfection protocol with 3 μg of a bicistronic shRNA plasmid (SuperArray, Bioscience Corp.) encoding a short hairpin silencing sequence (5′-TGTGTTGGAGGTTAA-GTACAT-3′). The bicistronic shRNA plasmid contains the shRNA under control of the U1 promoter and the EGFP cDNA to enable the identification of transfected myotubes. Silencing of the TRPC1 or TRPC4 gene was performed by means of the same transfection protocol using two different siRNA sequences (Eurogentec) against mouse TRPC1 mRNA (5′-GCAUCGUAUUUCACAUUCU-3′; 5′-UGAGCCUCUU-GACAAACGA-3′) or against the mouse TRPC4 mRNA (5′-CCCUUUCCUUACUGCCUU-3′; 5′-CGAGUUCACUG-AGUUUGU-3′).

Antibodies

Antibodies used against TRPC1 and TRPC4 (Sigma-Aldrich) were rabbit polyclonal antibodies, and those against α1-syntrophin were goat and rabbit polyclonal antibodies (Abcam, Cambridge, UK). Antibodies against dystrophin were rabbit polyclonal antibodies (Santa Cruz Biotechnology) and NCLDYS2 mouse monoclonal (Novocastra, Newcastle, UK). Others antibodies used were mouse monoclonal anti-c-Myc (Sigma-Aldrich) and mouse monoclonal anti-FLAG M2 antibody (Sigma-Aldrich). Secondary antibodies for immunofluorescence were Rhodamine Red-X-conjugated affinity-purified goat anti-rabbit IgG (Jackson ImmunoResearch) and FluoProbes 488 anti-mouse IgG antibodies (FluoProbes, Interchim, Montluçon, France). Secondary antibodies for Western blotting (Amersham Biosciences) were horseradish peroxidase-conjugated goat anti-mouse IgG and horseradish peroxidase-conjugated goat anti-rabbit IgG.

Pulldown Assays

Total cell lysates were obtained from minidys+ SolD6. Cells were washed three times in cold 1× TBS (20 mM Tris base, pH 7.4, 154 mM NaCl, 2 mM $MgCl_2$, 2 mM EGTA) and then lysed in 1 ml of radioimmune precipitation assay buffer (50 mM Tris-HCl, pH 7.4, 150 mM NaCl, 5 mM EDTA, 0.05% Nonidet P-40 (w/v), 1% deoxycholate (w/v), 1% Triton X-100 (v/v), 0.1% SDS (w/v)) in the presence of a 1% protease inhibitor mixture (1 mM phenylmethylsulfonyl fluoride, 20 mM leupeptin, 0.8 mM aprotinin, and 10 mM pepstatin). Protein lysates were homogenized by mechanical dissociation. The total protein concentration was measured by means of a Bio-Rad DC protein assay kit. Glutathione *S*-transferase (60 μg) or fusion protein consisting of GST and α1-syntrophin PDZ domain (60 μg) was incubated with 600 μg of cell lysates in a volume of NET solubilization buffer (50 mM Tris-HCl, pH 7.4, 150 mM NaCl, 5 mM EDTA, 0.05% Nonidet P-40 (v/v)) at 4 °C overnight with constant mixing followed by washing three times in NET. The bound proteins were eluted in an equal volume (20 μl) of loading buffer and heated for 5 min at 90 °C. The bound proteins were subjected to 10% SDS-PAGE, blotted, and probed with an anti-TRPC1 or anti-TRPC4 antibody.

Immunoprecipitation

After cell lysis, 2 μg of antibody was added to 200 μl of cell lysates diluted with 600 μl of NET solubilization buffer and incubated at 4 °C overnight with constant mixing. Then, the protein-antibody complex was incubated for 1 h at 4 °C with constant mixing with 40 μl of protein A/G-Sepharose (Amersham Biosciences). The immune complexes were collected by centrifugation and washed three times in NET. After denaturing, samples were subjected to SDS-PAGE, blotted with antibodies against dystrophin, TRPC1, TRPC4, c-Myc, and α1-syntrophin, probed for 1 h with 1:3000 horseradish peroxidase-conjugated anti-mouse or anti-rabbit antibodies (Amersham Biosciences), and developed with an enhanced chemiluminescence kit (Amersham Biosciences). The molecular weight of proteins was estimated according to prestained protein markers (Rainbow, Sigma-Aldrich).

Immunological Staining

The cultured cells were fixed in freshly made TBS, 4% paraformaldehyde for 20 min and permeabilized with TBS, 0.5% Triton X-100. A saturation step was executed with TBS, 1% BSA. Samples were incubated for 1 h with primary antibodies diluted in TBS, 1% BSA (20 mM Tris base, 154 mM NaCl, 2 mM EGTA, 2 mM $MgCl_2$, pH 7.5). After washing out in TBS, cells were incubated for 1 h in TBS, 1% BSA with secondary antibodies. The cells were mounted using Vectashield mounting medium (Vector Laboratories, Burlingame, CA). Muscle tissue was fixed by perfusion of TBS, 4% paraformaldehyde *in situ* for 30 min. Skeletal muscles were removed by dissection from 4-week-old mice and immediately fixed with 3% paraformaldehyde, 0.1 M phosphate buffer, pH 7.4, for 1 h at 4 °C. The fixed tissue was infused with a 30% sucrose solutions in PBS (20 mM phosphate buffer, pH 7.5, 150 mM NaCl) overnight at 4 °C. Cryosections of muscle fibers were immunolabeled overnight at 4 °C for indirect immunofluorescence with primary antibodies diluted at 2–5 μg/ml after 4 h in blocking solution (TBS, 1% BSA). The immunolabeled samples were examined using an Olympus IX71 epifluorescence microscope (Olympus, Tokyo, Japan), and confocal images were acquired by means of confocal laser scanning microscopy using an Olympus confocal system (confocal FV-1000 station). The maximal resolution was obtained with an Olympus UplanSapo ×60 water, 1.2 NA, objective lens. Fluorophores were excited with a 488-nm line of an argon laser (for fluorescein isothiocyanate), a 543-nm line of a HeNe laser (for TRITC). The emitted fluorescence was detected through spectral detection channels between 500 and 530 nm and 550 and 625 nm, for green and red fluorescence, respectively.

Measurement of Cation Influx Using Mn^{2+} Quenching of fura-2 Fluorescence

Myotubes at 3 or 4 days were rinsed with an external 1.8 Ca^{2+} solution (130 mM NaCl, 5.4 mM KCl, 1.8 mM $CaCl_2$, 0.8 mM $MgCl_2$, 10 mM HEPES, 5.6 mM D-glucose, pH 7.4, with NaOH) and incubated for 30 min in darkness and then for 15 min at 37 °C in the same solution supplemented with 3 μM (final concentration) fura-2/AM (FluoProbes). Loaded cells were washed with Ca^{2+}-free solution (130 mM NaCl, 5.4 mM KCl, 0.1 mM

EGTA, 0.8 mM $MgCl_2$, 10 mM HEPES, 5.6 mM D-glucose, pH 7.4, with NaOH) before measurements were made. fura-2 was excited at 360 nm with a Cairn monochromator (Cairn Research Ltd., Faversham, UK), and emission fluorescence was monitored at 510 nm using an intensified cooled charge-coupled device camera (Photonic Science Ltd., Robertsbridge, UK) coupled to an Olympus IX70 inverted microscope (×40 water immersion fluorescence objective). Transfected cells were located by EGFP fluorescence at 520 nm with excitation at 450 nm. The cation influx was evaluated by the quenching of fura-2 fluorescence at 360 nm when Mn^{2+} ions entered the cell. Fluorescence variations were recorded using Imaging Workbench 4.0 (IW 4.0) software (INDEC BioSystems, Mountain View, CA). The depletion protocol was three 1-min applications of 0 Ca^{2+}, 15 μM cyclopiazonic acid (reversible inhibitor of SERCA) alternating with three 1-min applications of free Ca^{2+}, 5 μM cyclopiazonic acid + 10 mM caffeine solution. The quench rate of the fluorescence intensity was estimated using linear regression of the decaying phase (slope) during the first 40 s after Mn^{2+} addition (50 μM, final concentration). The quench rate was expressed as percent/minute to correct for differences in the cell size or fluorophore loading. Statistical analysis was performed with Origin 5.0 software (OriginLab, Northampton, MA). No bleaching was observed during fluorescence measurements or a decrease of less than 0.5%/min. The difference between the mean values of measured parameters was tested statistically using the Student's *t* test and was considered significant at $p < 0.05$.

Membrane Potential Recordings

Membrane potential was recorded at room temperature from cultured myotubes using the whole-cell patch clamp technique. Glass micropipettes (2–5 megohms) were connected to the head stage of the patch clamp amplifier (Axopatch 200B, Axon Instruments, Foster City, CA) driven by an IBM PC-AT-compatible microcomputer equipped with an A/D-D/A conversion board (Digidata 1320A, Axon Instruments). Data acquisition and analysis were performed using the pCLAMP software package (Axon Instruments). Resting membrane potential (V_m) was recorded with the whole-cell patch clamp technique using the current clamp mode (current was clamped to zero). In this case, pipettes were filled with an internal medium containing (mM): 1 $MgCl_2$, 0.005 $CaCl_2$, 1 EGTA, 140 KCl, 10 HEPES, pH 7.2, with KOH. The external medium was composed of (mM): 0.8 $MgCl_2$, 1.8 $CaCl_2$, 5.6 glucose, 10 HEPES, 130 NaCl, 5.4 KCl, pH 7.4, with NaOH.

Reverse Transcription-PCR and Real-time PCR

Reverse Transcription—Total cellular RNA was extracted using RNABle kit (Eurobio). RNAs (10 μl) were reverse transcribed in 25 μl of reaction mixture consisting of first strand buffer (25 mM Tris, pH 8.3, 37.5 mM KCl, 1.5 mM $MgCl_2$), 10 mM dithiothreitol, 1 mM each dNTP, 2.4 mg of random hexamers, 40 units of RNase inhibitor (RNAguard, Amersham Biosciences), and 400 units of Moloney murine leukemia virus (M-MLV) reverse transcriptase (Invitrogen). Reverse transcription was performed at 37 °C for 60 min followed by 2 min at 100 °C. The solution was then diluted twice in water.

Real-time PCR—The 15-μl reaction mixture contained 7.5 μl of 2× TaqMan Universal Master Mix (Applied Biosystems), 5 μl of reverse transcription products, and the appropriate primers and probes (900 and 200 nM, respectively). All probes contained a 3′-6-carboxytetramethylrhodamine (TAMRA) quencher dye and were labeled at the 5′-end with a 6-carboxyfluorescein (FAM) reporter fluorescent dye. Amplification was performed at 50 °C for 2 min and then 95 °C for 10 min followed by 40 cycles at 95 °C (15 s) and 60 °C (1 min). Reactions were performed in MicroAmp optical 96-well reaction plates (Applied Biosystems) using an ABI PRISM 7700 sequence detection system (Applied Biosystems). All measurements were normalized to the mitochondrial ribosomal protein S6 (Mrps6, an endogenous control) to account for the variability in the initial concentration and quality of the total RNA.

For α1-syntrophin, the forward primer was 5′-ACT-GAC-CCA-GAG-CCC-AGG-TA-3′, and the reverse primer was 3′-TTG-GCC-CTC-AAG-AAG-ACA-GC-5′; the probe was 5′-6-FAM-CCT-GGC-CGT-CCG-CTG-CAC-AGA-T-3′-TAMRA. For SP6 protein control, the forward primer was 5′-TTT-GAT-TCT-GAA-AGC-CAT-GCG-3′, and the reverse primer was 3′-CGG-TCC-ATC-AGG-GAT-TCT-ATT-G-3′; the probe was 5′-6-FAM-CGG-CCA-GAG-ACC-GCT-GCT-GCT-3′-TAMRA.

RESULTS

siRNA Inhibition of α1-Syntrophin Expression Leads to Abnormal Increase of Divalent Cation Influx in Myotubes—To demonstrate that the expression level of α1-syntrophin at the sarcolemma is crucial for regulating cation influx, α1-syntrophin expression was repressed with siRNAs. Myoblasts were transfected with siRNA duplexes targeting α1-syntrophin mRNA, and 3-day differentiated minidys+ SolD6 myotubes were tested for expression levels of α1-syntrophin mRNA. We observed a drastic 93% extinction of the α1-syntrophin transcript value in cells transfected with siRNA against α1-syntrophin compared with cells transfected with a nontargeting siRNA pool (siRNA ghost) (Fig. 1*A*). The α1-syntrophin protein level was determined by Western blotting (Fig. 1*B*). The ratio of α1-syntrophin to mini-dystrophin (minidys) proteins was expressed as a percentage. Immunoblots showed that siRNA against α1-syntrophin decreased protein expression by 61% in transfected minidys+ SolD6 myotubes. The low expression of α1-syntrophin at the sarcolemma was confirmed by immunofluorescence labeling. α1-Syntrophin was detected at the sarcolemma of minidys+ SolD6 myotubes but not in samples obtained from cells transfected with siRNA against α1-syntrophin (Fig. 1*C*).

The impact of α1-syntrophin repression was tested on the association of this protein with dystrophin-based cytoskeleton. Minidys+ SolD6 muscle cells were transfected with siRNA against α1-syntrophin, and coimmunoprecipitation experiments were performed to isolate macromolecular complexes from 3-day myotubes. Protein extracts were incubated with anti-α1-syntrophin antibody for immunoprecipitation and probed with anti-dystrophin antibody (Fig. 2*A*, *upper panel*). The amount of mini-dystrophin coimmunoprecipitated with α1-syntrophin was decreased by 57% in siRNA-transfected myotubes. This result is in accordance with the diminu-

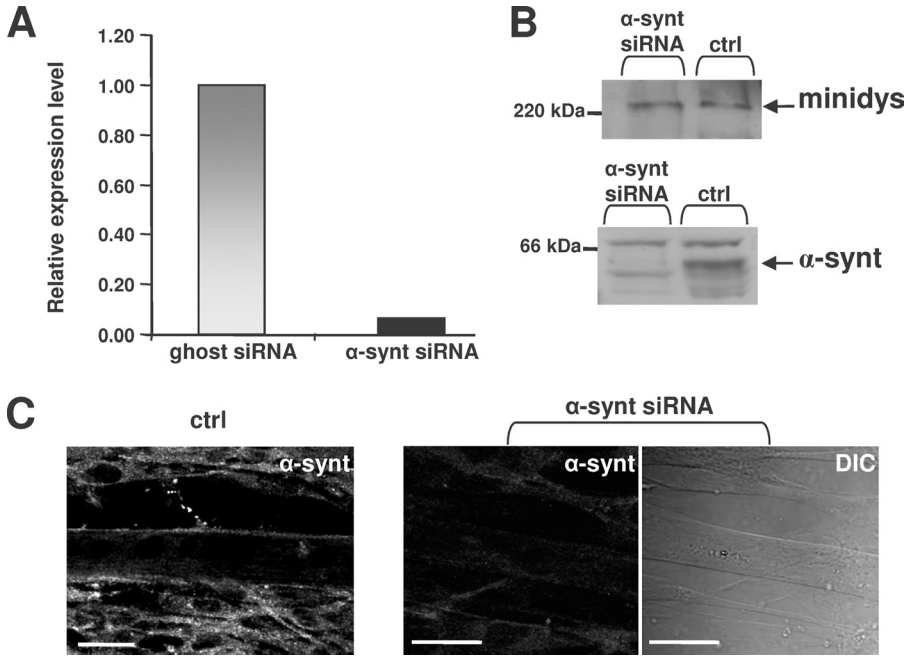

FIGURE 1. **Extinction of α1-syntrophin transcript and reduction of α1-syntrophin protein in minidys+ SolD6 myotubes.** *A*, 3-day differentiated minidys+ SolD6 muscle cells were harvested after transfection with siRNA against α1-syntrophin. *Bar graphs* represent the amount of α1-syntrophin mRNA analyzed by quantitative real-time PCR (value relative to the siRNA ghost control oligo). *B*, expression levels of α1-syntrophin in minidys+ SolD6 myotube control cells (*ctrl*) or in cells transfected with α1-syntrophin siRNA were analyzed by Western blots using an α1-syntrophin polyclonal antibody. The level of α1-syntrophin was compared with that of mini-dystrophin detected with a polyclonal antibody. *C*, immunofluorescence microscopy of minidys+ SolD6 myotubes transfected with α1-syntrophin siRNA. The *right panel* represents a phase contrast picture of the same α1-syntrophin siRNA-transfected cells in the *central panel*. *Bars* = 10 μM.

tion of α1-syntrophin protein expression shown in Fig. 2*A*, *lower panel*. The drastic extinction of α1-syntrophin is accompanied by a loss of TRPC1-α1-syntrophin complex, as shown by the absence of TRPC1 immunoprecipitated with α1-syntrophin (Fig. 2*B*).

Minidys+ SolD6 myotubes were transfected with siRNA against α1-syntrophin to determine the impact of the loss of α1-syntrophin on cation influxes after 3 days of differentiation. Divalent cation entry was stimulated after partial store depletion by the repetitive activation of calcium release by caffeine (10 mM) in the presence of cyclopiazonic acid, a SERCA inhibitor. After the stores were depleted by this procedure, 50 μM manganese ions were readmitted in the extracellular space, which induced a store-operated influx of divalent cations reflected by the progressive quenching of fura-2 fluorescence by Mn^{2+} (Fig. 2*C*). All values of the quenching rate were expressed as absolute values. This divalent cation entry was shown previously to be blocked by 40 μM SKF-96365, a cation channels inhibitor (7). It must be noted that when 50 μM manganese ions were readmitted without depletion of the stores, a Mn^{2+}-decreasing phase of fura-2 fluorescence was recorded (6.0%/min ± 0.2, $n = 131$ in nonstimulated minidys+ SolD6 myotubes), which was not affected by SKF-96365 (data not shown). This influx is represented in all *bar graphs* under the *dotted line* (Fig. 2*D*, Fig. 3*E*, and Fig. 5, *B*, *D*, and *E*). The values of cationic influx are thus the result of a store-operated cation entry sensitive to SKF-96365 and of a background cation entry insensitive to SKF-96365. After depletion, the resulting divalent cation entries were greatly increased in transfected cells with α1-syntrophin siRNA (24%/min ± 0.9, $n = 81$) as compared with untransfected SolD6 myotubes (control cells; 13.5%/min ± 0.5, $n = 74$) or with transfected cells with a nontargeting siRNA pool (15.1%/min ± 0.6, $n = 28$) (Fig. 2*D*). Incidentally, α1-syntrophin silencing led to divalent cation influx, which tended to reach levels similar to the cation influxes recorded in dystrophin-deficient cells (dys− SolC1; 28.1%/min ± 0.8, $n = 115$). A shRNA plasmid encoding a silencing shRNA targeted to another sequence of α1-syntrophin mRNA was also used to rule out off-target effects. Transfection with the shRNA plasmid also resulted in expression of EGFP, which allowed us to identify transfected cells. When transfection resulted in 30% of the myotubes expressing EGFP, quantification of α1-syntrophin by immunoblots performed on total protein lysate showed a 35% decrease in the protein level. The cation influx was recorded on shRNA-transfected myotubes expressing EGFP (data not shown). The analysis of these recordings showed an 86% increase in divalent cation influx, which is similar to the results obtained after silencing with siRNA (77% increase). These data demonstrate that the loss of α1-syntrophin severely increases divalent cation entry in muscle cells and alters regulation by mini-dystrophin. This result suggests a crucial role of α1-syntrophin in the regulation of cation influx by the dystrophin-based cytoskeleton.

Requirement of α1-Syntrophin PH1a and PDZ Domains (N Terminus) for Regulation of Divalent Cation Entry in Myotubes—The syntrophins are a family of scaffolding proteins that contain four distinct domains (Fig. 3*A*). The N-terminal part contains a half-PH1a domain and a PDZ domain. Expression vector ΔN-α1-syntrophin-EGFP (Fig. 3*A*, Δ*N-α-synt*) was developed; this encodes for a truncated α1-syntrophin lacking the PH1a and PDZ domains with the aim of evaluating the functional role of those domains.

Immunostaining of α1-syntrophin was performed to estimate the overexpression of the truncated protein ΔN-α-synt in transfected minidys+ SolD6 myotubes compared with untransfected cells and to observe its localization despite the absence of the N-terminal of α1-syntrophin. When transfected, ΔN-α1-syntrophin was clearly concentrated at the sarcolemma (Fig. 3*B*), as well as the staining of transfected FL-α1-syntrophin (Fig. 3*C*), whereas EGFP expression was observed in the cytoplasm. The immunofluorescent staining of ΔN-α1-syntrophin was strongly increased at the sarcolemma as compared with the staining obtained from endogenous α1-syntrophin (Fig. 3*D*). Despite the absence of the N-terminal part, it appears that the truncated α1-syntrophin is

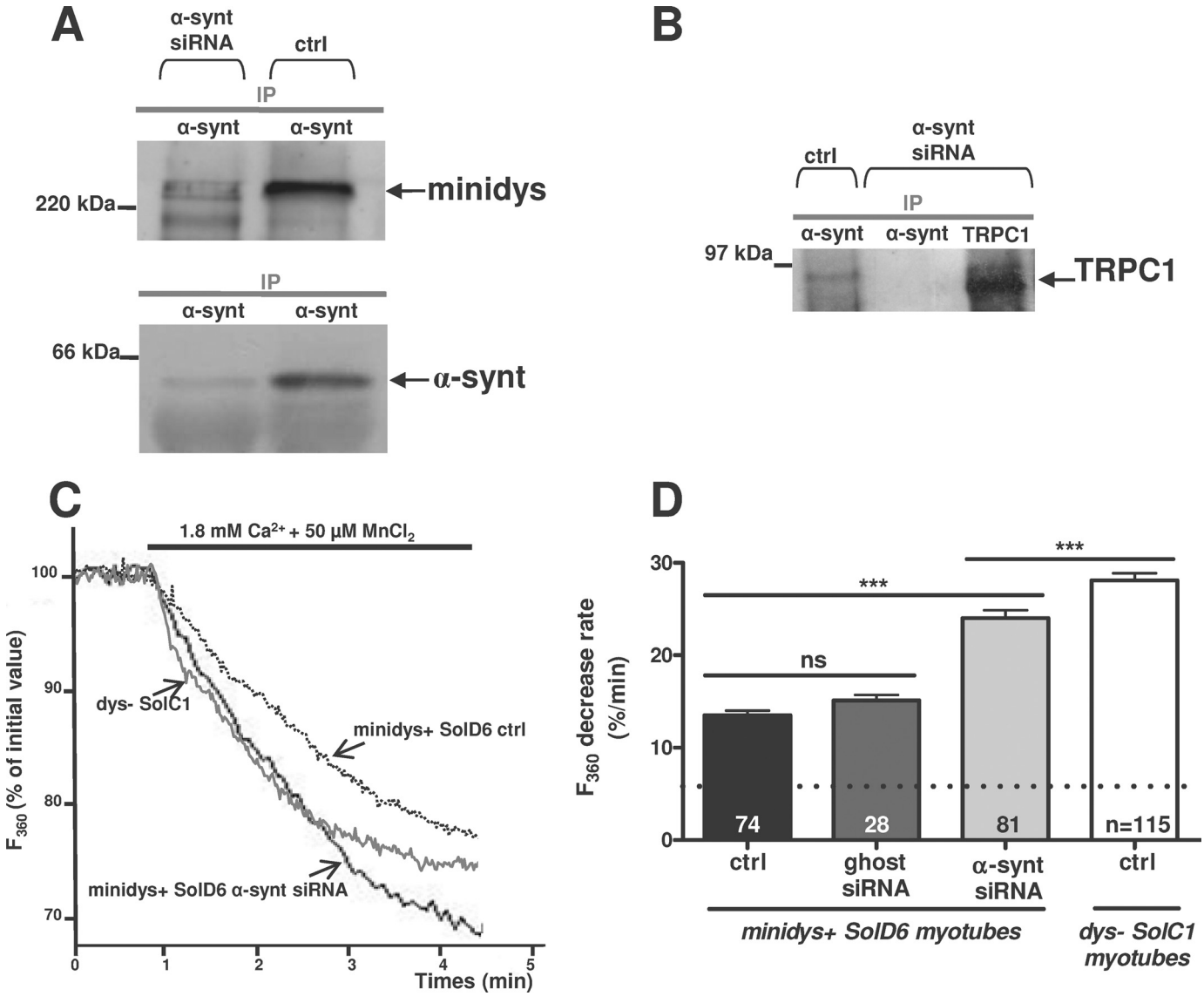

FIGURE 2. **α1-Syntrophin is essential for normal regulation of cation entry in cultured myotubes.** *A*, protein lysates from minidys+ SolD6 myotubes transfected with siRNA against α1-syntrophin or from untransfected cells (control (*ctrl*)) were incubated with polyclonal antibody raised against α1-syntrophin (*α-synt lane*). Western blots of the immunoprecipitated proteins (*IP*) were probed with a polyclonal antibody against mini-dystrophin and a polyclonal antibody against α1-syntrophin. *B*, protein lysates from minidys+ SolD6 myotubes transfected with siRNA against α1-syntrophin or from untransfected cells were incubated with polyclonal antibody raised against TRPC1 and α1-syntrophin. Western blots of the immunoprecipitated proteins were probed with a polyclonal antibody against α1-syntrophin and a polyclonal antibody against TRPC1. *C*, three representative recordings of fura-2 fluorescence during perfusion of 50 μM Mn^{2+} obtained from nontransfected minidys+ SolD6 myotubes (*dotted line*), from a minidys+ SolD6 myotubes transfected with siRNA against α1-syntrophin (*bolder gray line*), and from a dystrophin-deficient SolC1 myotubes (*gray line*). *D*, slopes of the Mn^{2+}-induced decreasing phase of fura-2 fluorescence were measured and expressed as percent decrease/min. *Bar graphs* represent mean rates of fluorescence decrease induced by Mn^{2+} (expressed in %/min) ± S.E. in control SolD6 myotubes (*black column*), in control SolD6 myotubes transfected with siRNA ghost (*dark gray column*), and in SolD6 transfected with α1-syntrophin siRNA (*light gray column*). The *white column* represents abnormally elevated cation entry in dys− SolC1 myotubes. The difference between mean values of measured parameters was determined by Student's *t* test and considered significant at $p < 0.05$ (***, $p < 0.001$). The cationic influx measured under the *dotted line* represents the background cation entry insensitive to SKF-96365. *n.s.*, no significant.

normally targeted to the sarcolemma of myotubes expressing dystrophin.

The truncated α1-syntrophin was transiently transfected in normal minidys+ SolD6 myotubes (Fig. 3*E*) and also in dystrophic dys− SolC1 myotubes (Fig. 3*F*); the consequences for cation influx were explored by measuring store-operated divalent cation influx in myotubes 4 days after initiation of differentiation. The green fluorescence of myotubes was used to identify transfected cells with pCMS-enhanced GFP plasmid expressing both EGFP and recombinant ΔN-α1-syntrophin independently. No significant variations in the rate of quenching of fura-2 (reflecting divalent cation entry) were observed in control minidys+ SolD6 myotubes expressing recombinant ΔN-α-synt (15.8%/min ± 0.9, $n = 52$) compared with untransfected cells (14.7%/min ± 0.4, $n = 124$). As described previously, dystrophin-deficient myotubes displayed higher levels of cation influx than myotubes expressing mini-dystrophin (7). Forced expression of ΔN-α-synt in dystrophin-deficient myotubes did not reduce divalent cation influx (25.5%/min ± 1.5, $n = 30$) as compared with untransfected dystrophin-deficient SolC1 myotubes (28.1%/min ± 0.8, $n = 115$). By contrast, the cation influx was significantly reduced into myotubes transfected with FL-

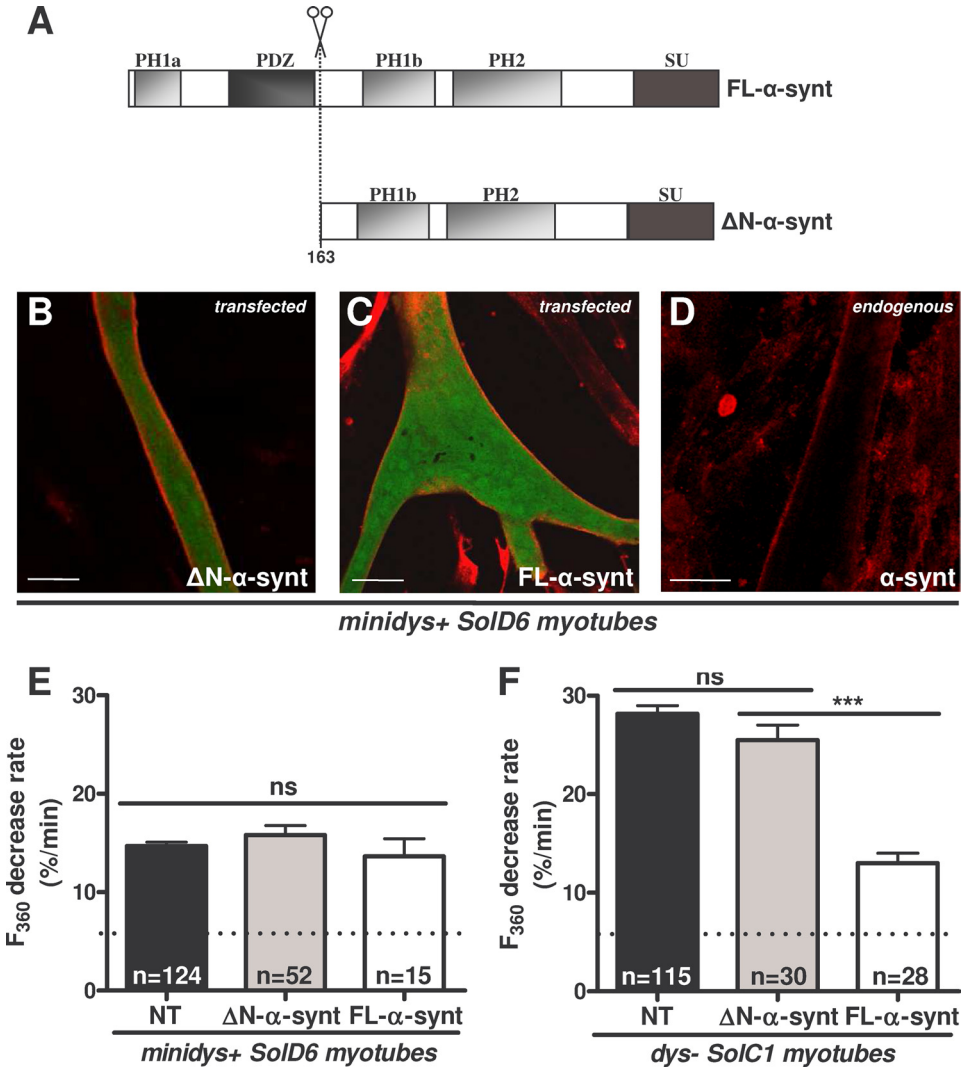

FIGURE 3. **The N terminus corresponding to the PH1a and PDZ domains of α1-syntrophin is necessary for regulating the abnormally elevated cation entry in dystrophin-deficient cultured myotubes.** *A*, structural diagram of FL-α1-syntrophin and α1-syntrophin missing the PH1a and PDZ domains (Δ*N*), showing the relative localization of the PH domains, the PDZ domain, and the syntrophin-unique domain. *B–D*, differentiated minidys+ SolD6 myotubes were transfected with plasmids encoding ΔN-α1-syntrophin-EGFP and FL-α1-syntrophin-EGFP. Myotubes were immunostained with antibody specific for α1-syntrophin (in *red*). EGFP expression in cytoplasm is shown in *green*. The expression level of α1-syntrophin was evaluated by the intensity of red fluorescence. *Bars* = 10 μM. *E* and *F*, minidys+ SolD6 and dys− SolC1 myotubes were transfected with the expression vector encoding ΔN-α1-syntrophin-EGFP. *E*, mean rates of fluorescence decrease induced by Mn^{2+} (expressed in %/min) ± S.E. in minidys+ SolD6 myotubes transfected (*gray column*) with the ΔN-α1-syntrophin-EGFP or nontransfected (*NT*, *black column*). *ns*, not significant. *F*, same experiment as in *E* on dys− SolC1 myotubes. The *white columns* represent results of the effect of FL-α1-syntrophin forced expression on cation entry, which confirms those already reported by Vandebrouck *et al.* (7).

α1-syntrophin (13.0 ± 1.0, $n = 28$). The results obtained with FL-α1-syntrophin confirmed our previous observation in Vandebrouck *et al.* (7). These data suggest that the N-terminal part of α1-syntrophin mediates the regulation of cation entry in muscle cells.

Endogenous TRPC4 Interacts with Sarcolemmal TRPC1 in Muscle and Cultured Myotubes—The formation in skeletal muscle cells of heterotetrameric channels associating TRPC1 and TRPC4 was explored because the use of antisense had suggested previously that store-operated calcium currents recorded in fibers are dependent on the expression level of TRPC1 and TRPC4 channels (22). Moreover, TRPC1 translocation into the plasma membrane has been shown to depend upon the expression of TRPC4 at the membrane (32). Fig. 4*A* shows representative images obtained with confocal fluorescence microscopy that illustrate TRPC4 and TRPC1 localization in differentiated minidys+ SolD6 myotubes, in myotubes from C57BL/10 mice primary cultures, and in C57BL/10 fibers. Higher magnifications revealed strong staining along the sarcolemma and punctuate intracellular staining of TRPC4 and TRPC1 in myotubes. Substantial staining of TRPC1 in a striated pattern was observed in muscle fibers, and TRPC4 and TRPC1 were also distributed along the sarcolemma as shown by the costaining of dystrophin (Fig. 4*A*), which is in agreement with data described previously (22). These immunostainings show that these two types of channels are localized at the same sarcolemmal area in skeletal muscle and may form plasma membrane channels associated with costameres.

This result illustrates sarcolemmal localization of TRPC4 and TRPC1, which suggests a possible molecular association. To demonstrate that TRPC1 and TRPC4 form a complex in muscle cells, we performed coimmunoprecipitation assays. Western blots probed with TRPC1 and TRPC4 antibodies (Fig. 4*B*) revealed that TRPC1 was coimmunoprecipitated with TRPC4 (*IP lane*: *TRPC4*) and conversely that TRPC4 was coimmunoprecipitated with TRPC1 (*IP lane*: *TRPC1*) in normal C57BL/10. These results show that TRPC1 and TRPC4 form a stable complex in muscle cells and may form a heterotetrameric channel along the sarcolemma.

TRPC1 and TRPC4 Are Involved in Divalent Cation Influx in Cultured Myotubes—To determine whether TRPC1 and TRPC4 support the store-operated cation entry recorded in skeletal muscle cells, we first used an overexpression strategy and secondly an RNA interference strategy to decrease endogenous TRPC mRNA levels with further assessments of its impact on cation influx.

Exogenous Myc-tagged TRPC4 and FLAG-tagged TRPC1 were transfected in minidys+ SolD6 myotubes and consequently immunostained with goat anti-mouse Alexa 488 secondary antibody. The staining of TRPC1 and TRPC4 was enriched along the sarcolemma of the myotubes, confirming

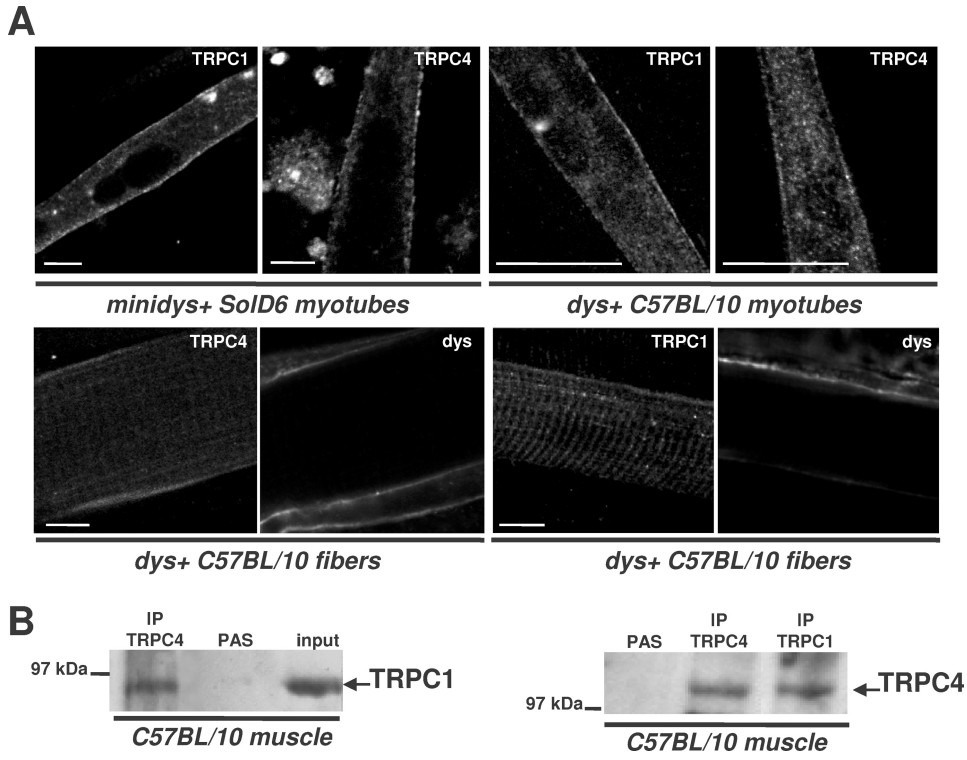

FIGURE 4. **TRPC4 and TRPC1 are present at the sarcolemma of muscle and cultured myotubes and form a stable complex in skeletal muscle.** *A*, laser scanning confocal microscopy analysis of TRPC1 and TRPC4 distribution. Immunostaining in minidys+ SolD6 cultured myotubes, in dys+ C57BL/10 myotubes from primary cultures, and in C57BL/10 skeletal muscle (*semi-thin section*) is shown. Costaining of dystrophin in skeletal muscle was obtained with a mouse monoclonal antibody to show the cortical compartment of muscle fibers. *Bars* = 10 μM. *B*, muscle lysates were incubated with polyclonal antibodies against TRPC1 (*IP*: *TRPC1 lane*) or TRPC4 (*IP*: *TRPC4 lane*). Immunoprecipitation was carried out with protein A-Sepharose beads (*PAS*). Western blot of the immunoprecipitated proteins was probed with polyclonal antibodies against TRPC1 or TRPC4. Positive controls for immunoprecipitation were carried out with antibodies raised against TRPC1 or TRPC4, respectively, and negative controls were performed with protein A-Sepharose.

that TRPC1 and TRPC4 form channels at the sarcolemmal compartment (Fig. 5*A*).

Myoblasts were co-transfected using Nucleofector technology (Amaxa) with FLAG-tagged TRPC1 or Myc-tagged TRPC4 plasmids and a plasmid expressing only EGFP (called pmaxGFP) with a ratio of 1 μg of pmaxGFP to 4 μg of FLAG-tagged TRPC1 or Myc-tagged TRPC4. The GFP plasmid was used to identify transfected myotubes with TRPC1 and TRPC4. As shown in Fig. 5*A*, the distribution of transfected TRPC1-FLAG and TRPC4-Myc was examined in minidys+ SolD6 myotubes, presenting a clear concentration of these proteins at the sarcolemma.

Divalent cation influx was explored after the recombinant TRPC1 or TRPC4 was transiently transfected in minidys+ SolD6 myotubes (Fig. 5*B*). The recordings of store-operated divalent cation influxes showed a large increase in divalent cation entry in myotubes expressing either recombinant TRPC1 (24.3%/min ± 1.8, $n = 16$) or TRPC4 (22.8%/min ± 1.9, $n = 28$) compared with control myotubes (14.7%/min ± 0.4, $n = 124$). Therefore, overexpression of TRPC1 and TRPC4 appears to enhance the divalent cation influx recorded in myotubes stimulated by a store depletion protocol.

Moreover, cultured myoblasts were transfected by nucleofection with siRNA against TRPC1 and, on the other hand, with siRNA against TRPC4 (Fig. 5*C* and *D*). The consequences for the protein level and for store-operated cation entry were explored, respectively, by Western blot (Fig. 5*C*) and by measuring cation influx in differentiated myotubes 3 days after initiation of differentiation (Fig. 5*D*). Western blot analysis showed a large decrease in TRPC1 expression by 89% and TRPC4 expression by 84% in minidys+ SolD6 myotubes transfected with TRPC1 and TRPC4 siRNAs compared with control cells, confirming TRPC1 and TRPC4 knockdown at the protein level.

Alterations of endogenous TRPC1 protein appeared to decrease store-operated cation influx (TRPC1 siRNA: 9.3%/min ± 0.5, $n = 42$) as well as TRPC4 siRNA (9.5%/min ± 0.7, $n = 27$) compared with the control cell values (13.5%/min ± 0.5, $n = 74$). In other words, TRPC1 knockdown resulted in a 31% inhibition of divalent cation influx in myotubes. Similarly, TRPC4 silencing resulted in a 30% inhibition of divalent cation influx. This shows that at least part of the divalent cation influx recorded in myotubes after store depletion was supported by TRPC1 and TRPC4. Taking into account the background non-store-operated cation entry recorded in nondepleted myotubes (6.0%/min), the remaining store-operated component of cation entry was 41 and 44% after TRPC1 and TRPC4 knockdown, respectively (Fig. 5*D*). This remaining component after siRNA treatment could be supported by residual TRPC1 and TRPC4 expression or other types of store-operated channels. To rule out off-targets effects, two different siRNAs designed against different targets in TRPC1 and TRPC4 mRNA were used, giving similar results in the inhibition of divalent cation entry (not shown).

These results further suggest that TRPC1 and TRPC4 comprise an important subunit of functional native divalent cation channels in cultured myotubes and that this influx is dependent on store depletion. TRPC1 was shown to form a SOC with STIM1 and Orai1, which is inhibited by 1 μM Gd^{3+} (17). To understand the involvement of STIM/Orai in the influx recorded in cultured myotubes, 1 μM Gd^{3+} was used to inhibit STIM/Orai pathway. The divalent cation influx measured after store depletion was insensitive to 1 μM Gd^{3+} (supplemental Fig. S2). Similarly, this inhibitor had no effect on abnormal cation influx measured in minidys+ SolD6 transfected with α1-syntrophin siRNA. On the contrary, administration of 10 μM Gd^{3+} (a powerful inhibitor of cation channels) led to a drastic reduction of cation influx (supplemental Fig. S2).

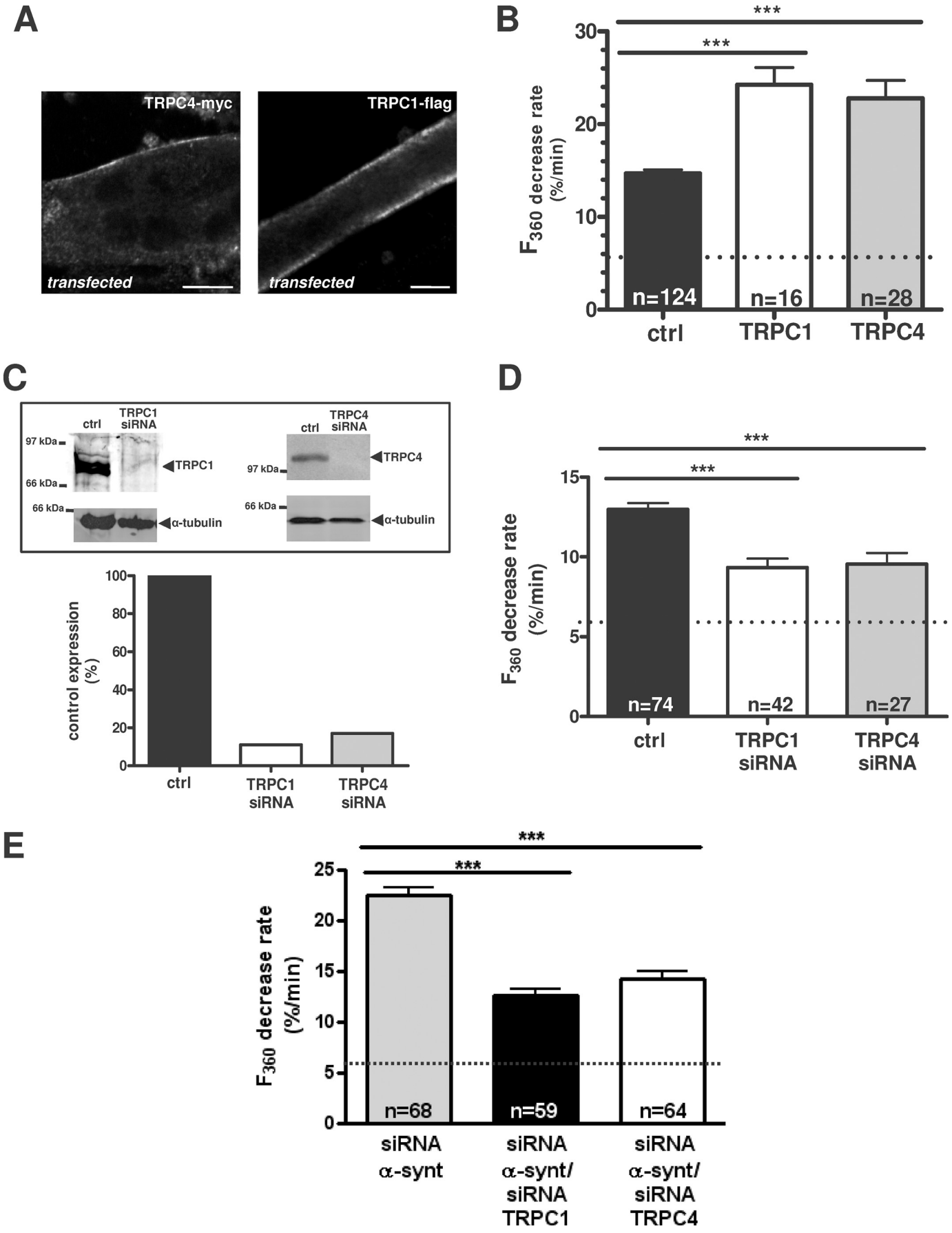
A
TRPC4-myc
transfected
TRPC1-flag
transfected
B
***
***
F360 decrease rate (%/min)
30
20
10
0
n=124
n=16
n=28
ctrl
TRPC1
TRPC4
C
ctrl
TRPC1 siRNA
97 kDa
66 kDa
TRPC1
66 kDa
α-tubulin
ctrl
TRPC4 siRNA
97 kDa
TRPC4
66 kDa
α-tubulin
control expression (%)
100
80
60
40
20
0
ctrl
TRPC1 siRNA
TRPC4 siRNA
D
***
***
F360 decrease rate (%/min)
15
10
5
0
n=74
n=42
n=27
ctrl
TRPC1 siRNA
TRPC4 siRNA
E
***
***
F360 decrease rate (%/min)
25
20
15
10
5
0
n=68
n=59
n=64
siRNA α-synt
siRNA α-synt/ siRNA TRPC1
siRNA α-synt/ siRNA TRPC4

To determine whether the two isoforms of TRPC were involved in the divalent cation entry regulated by the expression of α1-syntrophin, experiments with double siRNAs against α1-syntrophin and TRPC1, as well as with siRNAs against α1-syntrophin and TRPC4, were performed in minidys+ SolD6 myotubes. Reduction of the protein level was confirmed by Western blot after double silencing (not shown). The quenching results shown in Fig. 5*E* demonstrate that the abnormal influxes measured when α1-syntrophin was knocked down (24.0%/min ± 0.9, $n = 81$) were decreased after double extinction of either α1-syntrophin and TRPC1 (12.6%/min ± 0.6, $n = 59$) or α1-syntrophin and TRPC4 (14.2%/min ± 0.7, $n = 64$). The repression of TRPC1 or TRPC4 counteracted the increase of cation influx resulting from repression of α1-syntrophin. Therefore, these data clearly show that divalent cation entry regulated by α1-syntrophin expression level is dependent on both TRPC1 and TRPC4 in cultured myotubes.

L-type Calcium Channels Are Not Involved in Divalent Cation Influx—To discriminate non-voltage-dependent calcium channels from voltage-dependent calcium channels, nifedipine (5 μM) was used to selectively block calcium L-type components (ICa_L). Nifedipine was administrated at the same time as Mn^{2+} solution. The divalent cation influx measured after store depletion was insensitive to nifedipine (supplemental Fig. S1), as shown by the absence of effect of this compound on the divalent cation influx recorded in minidys+ SolD6 myotubes (14.5%/min ± 0.9, $n = 76$ with nifedipine and 14.7%/min ± 0.4, $n = 124$ in the control). On the contrary, a large component of divalent cation influx was sensitive to 40 μM SKF-96365, a store-operated channel inhibitor, in minidys+ SolD6 myotubes (7.6%/min ± 0.5, $n = 41$). This pharmacological tool demonstrates that ICa_L does not participate in cation entry under these experimental conditions. Moreover, we recorded the resting membrane potential after the depletion protocol in minidys+ SolD6 myotubes and obtained a mean value of −61 mV. The depletion protocol leads to low depolarization (around 6 mV depolarization for minidys+ SolD6 and around 4 mV depolarization for dys−SolC1), but the membrane potential remains underneath the activation threshold of L-type calcium channels, which is normally around −30 mV in human (34, 35) and rat (36) myotubes and in wild type fibers (37). Nifedipine was used in minidys+ SolD6 transfected with α1-syntrophin siRNA (supplemental Fig. S1). Nifedipine had no effect on abnormal cation influx measured when α1-syntrophin expression was inhibited (25%/min ± 2.1, $n = 43$). This shows that in absence of α1-syntrophin, the abnormal cation influx is not due to L-type calcium channel activity. Moreover, the knockdown of α1-syntrophin in minidys+ SolD6 transfected with α1-syntrophin siRNA did not significantly change the resting membrane potential. Indeed, the resting potential was slightly more negative compared with control minidys+ SolD6 (around 3 mV hyperpolarization). It is interesting to note that in dystrophin-deficient myotubes, the resting potential was also more negative compared with minidys+ SolD6 myotubes (around 8 mV hyperpolarization). The values of membrane potential in cultured myotubes are represented in supplemental Table 1.

TRPC4 Is Associated with the α1-Syntrophin/Dystrophin-based Cytoskeleton in Muscle and Cultured Myotubes—The plasmid encoding for FL-α1-syntrophin-Myc was transfected in minidys+ SolD6 muscle cells in order to explore the interaction of the scaffolding protein with endogenous TRPC4. Protein lysates were incubated with anti-TRPC4, anti-dystrophin, and anti-Myc antibodies for immunoprecipitation and probed with anti-Myc antibody. Fig. 6*A* shows that the recombinant α1-syntrophin coimmunoprecipitated with TRPC4, which suggests that recombinant α1-syntrophin forms a macromolecular complex with endogenous TRPC4 in cultured myotubes. TRPC4 contains a conserved sequence at the C-terminal (three amino acids, TRL (38)), which suggests that TRPC4 may interact with a common PDZ domain. Therefore, we tested whether TRPC4, like TRPC1 (7), interacts with the α1-syntrophin PDZ domain. Fig. 6*B* shows that TRPC4 from lysates of minidys+ SolD6 myotubes can bind to GST fusion protein containing the PDZ domain of α1-syntrophin like TRPC1 from the same lysates (Fig. 6*B*). To test whether endogenous TRPC4 associates with α1-syntrophin and dystrophin in muscle cells, we looked for this complex by using coimmunoprecipitation assays with lysates from C57BL/10 and from cultured myotubes.

Fig. 6*C* represents immunoblots revealed by polyclonal TRPC4 and TRPC1 antibodies. A band of around 117 kDa, corresponding to TRPC4, was detected in the anti-dys, anti-α-synt, and anti-TRPC1 precipitates from C57BL/10 muscle. Conversely, the immunoblot revealed by polyclonal TRPC1 antibody demonstrates a band of around 90 kDa corresponding to TRPC1 with anti-dys, anti-α-synt, and anti-TRPC4 precipitates. These results clearly show that endogenous TRPC4 interacts with TRPC1 channels in C57BL/10 muscle cells but also with the dystrophin-α1-syntrophin complex. It shows for the first time that mature mice muscles have a macromolecular complex containing TRPC1 and TRPC4 channels linked to the

FIGURE 5. **TRPC1 and TRPC4 are involved in cation influx regulated by α1-syntrophin in minidys+ SolD6 myotubes.** *A*, analysis by laser scanning confocal microscopy of Myc-tagged TRPC4 and FLAG-tagged TRPC1 immunostaining in transfected minidys+ SolD6 cultured myotubes. *Bars* = 10 μM. *B*, minidys+ SolD6 myotubes were transfected with the expression vector encoding TRPC1 or TRPC4. Mean rates of fluorescence decrease induced by Mn^{2+} (expressed in %/min) ± S.E. are shown in control minidys+ SolD6 myotubes (*ctrl*; *black column*) and in minidys+ SolD6 transfected with TRPC1 (*white column*) and TRPC4 (*gray column*). The difference between mean values of measured parameters was processed by Student's *t* test and considered significant at $p < 0.05$ (***, $p < 0.001$). *C*, histograms show efficiency of TRPC1 and TRPC4 expression after siRNA treatment. TRPC1 and TRPC4 protein levels were normalized to α-tubulin and expressed as percent of control. *D*, effect of siRNA knockdown of individual TRPC homologues on store-operated cation entry. Minidys+ SolD6 were transfected with TRPC1 or TRPC4 siRNA. Mean rates of fluorescence decrease induced by Mn^{2+} (expressed in %/min) ± S.E. are shown in control minidys+ SolD6 myotubes (*black column*) and in minidys+ SolD6 transfected TRPC1 siRNA (*white column*) and TRPC4 siRNA (*gray column*). The difference between mean values of measured parameters was determined by Student's *t* test and was considered significant at $p < 0.05$ (***, $p < 0.001$). *E*, effect of double siRNA knockdown of α1-syntrophin and TRPC1 and, on the other hand, of α1-syntrophin and TRPC4 on store-operated cation influx in minidys+ SolD6 myotubes. Mean rates of fluorescence decrease induced by Mn^{2+} (expressed in %/min) ± S.E. are shown in minidys+ SolD6 myotubes transfected with α1-syntrophin siRNA (*gray column*) and in minidys+ SolD6 transfected with double siRNAs against α1-syntrophin/TRPC1 (*black column*) and double siRNAs against α1-syntrophin/TRPC4 (*white column*). The difference between mean values of measured parameters was analyzed by Student's *t* test and considered significant at $p < 0.05$ (***, $p < 0.001$).

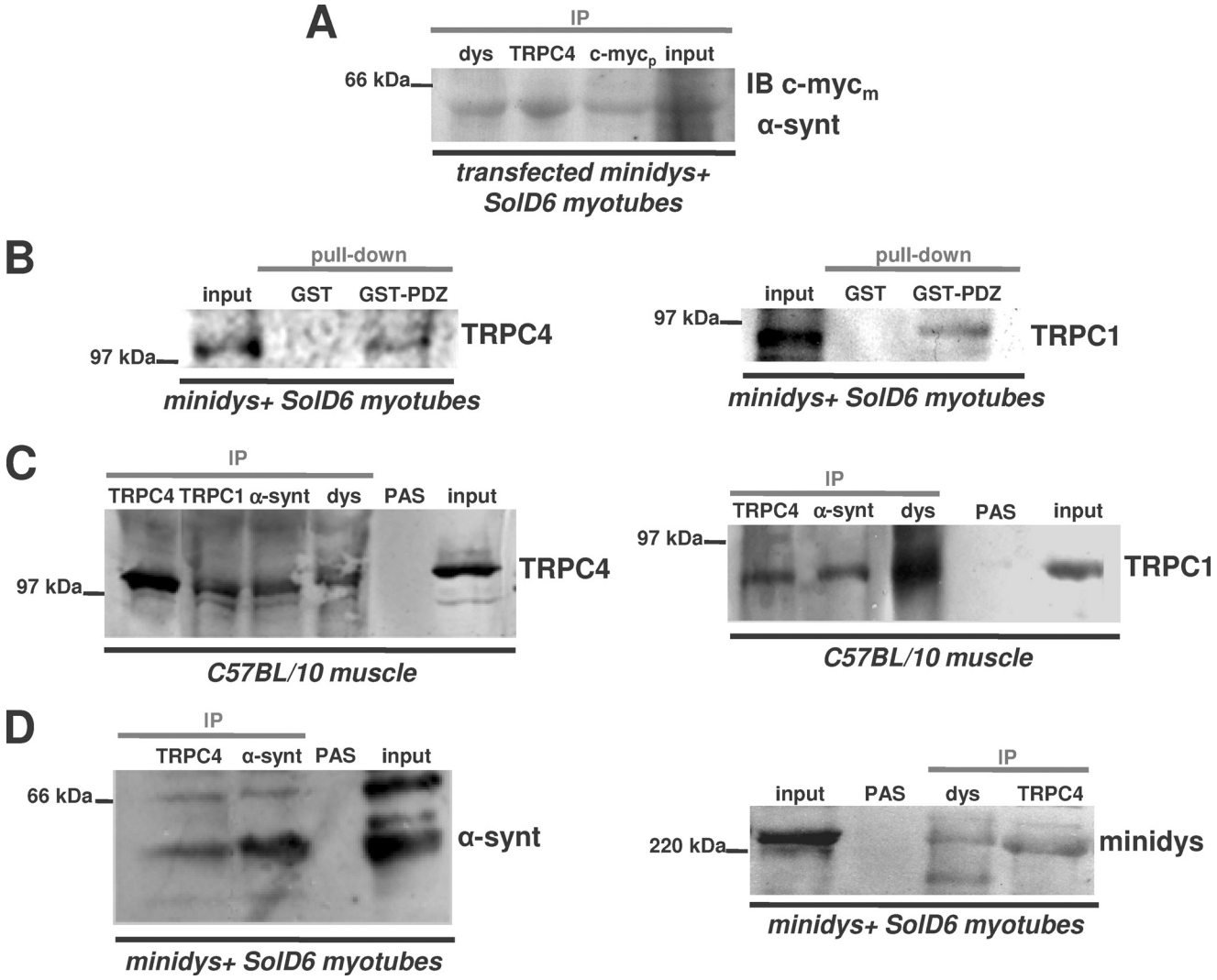

FIGURE 6. **TRPC4 associates *in vitro* with the PDZ domain of α1-syntrophin and forms a macromolecular complex with TRPC1, dystrophin, and α1-syntrophin in skeletal muscle and cultured myotubes.** *A*, the lysates from differentiated minidys+ SolD6 myotubes transfected with FL-α1-syntrophin-c-Myc-EGFP plasmid were immunoprecipitated (*IP*) with polyclonal antibodies against c-Myc tag (*c-Myc$_p$ lane*), TRPC4 (*TRPC4 lane*), and dystrophin (*dys lane*). The resulting immunoblot (*IB*) was probed with a monoclonal antibody against c-Myc tag (*c-Myc$_m$*). *B*, beads charged with GST alone or with a GST fusion protein of the PDZ domain of α1-syntrophin were incubated with protein lysates from minidys+ SolD6 myotubes. Bound proteins were immunoblotted with a polyclonal TRPC4 antibody or with a polyclonal TRPC1 antibody. The *input lane* was loaded with 10% of the extract used for the pulldown. *C*, muscle lysates from C57BL/10 muscles (*input lane*) were incubated with polyclonal antibodies against dystrophin (*dys lane*), α1-syntrophin (*α-synt lane*), TRPC1 (*TRPC1 lane*), and TRPC4 (*TRPC4 lane*). Western blots of the immunoprecipitated proteins were probed with polyclonal antibodies against TRPC4 or TRPC1. *PAS*, protein A-Sepharose. *D*, protein lysates (*input lane*) from minidys+ SolD6 myotubes were incubated with polyclonal antibodies against α1-syntrophin, TRPC4, and mini-dystrophin (*dys lane*). Western blots of the immunoprecipitated proteins were probed with polyclonal antibodies against α1-syntrophin or mini-dystrophin.

cytoskeletal dystrophin-α1-syntrophin complex. Fig. 6*D* shows immunoblots of α1-syntrophin and dystrophin in minidys+ SolD6 myotubes. A band corresponding to α1-syntrophin was present with the immunoprecipitate of TRPC4, and a band corresponding to the 230-kDa mini-dystrophin was detected in the immunoprecipitate of TRPC4. These results are in agreement with those of Fig. 6*C*. In cultured cells expressing mini-dystrophin, a macromolecular complex is constituted between mini-dystrophin, α1-syntrophin, and endogenous TRPC4 as well as TRPC1 (7). The same macromolecular complex is formed in mini-dystrophin-expressing myotubes as in mature muscles.

DISCUSSION

In this study, we present new evidence for a crucial role of α1-syntrophin in regulating TRPC1- and TRPC4-dependent cation influx in skeletal muscle cells. We demonstrate the interaction of TRPC1 and TRPC4 channels with α1-syntrophin and the PDZ domain. Moreover, we show the requirement of this domain and of the presence of α1-syntrophin in the DAPC for normal regulation of TRPC-dependent cation entry.

Several studies performed with dystrophin-deficient mice or human muscles have suggested that the DAPC regulates the activity of sarcolemmal cation channels responsible of sustained calcium influx (39). Among these voltage-independent channels with higher activity in dystrophin-deficient muscle, TRPC1 and TRPC4 (22) have been shown to support sarcolemmal calcium currents that are spontaneously active and also are activated by treatment with thapsigargin or caffeine. We showed previously that in dystrophin-deficient myotubes displaying higher cation entry, transfected mini-dystrophin form a

complex with TRPC1 and α1-syntrophin and reduce the cation influx (7). Transfection of a recombinant α1-syntrophin was also shown to reduce abnormal cation entry in dystrophin-deficient muscle cells, suggesting that recombinant α1-syntrophin restores the regulation of cation channels independently of dystrophin.

We show here that the regulation obtained with full-length α1-syntrophin is lost when the N-terminal part of the scaffolding protein is deleted, which suggests a specific role of the PDZ domain. Moreover, a recombinant GST-PDZ domain of the scaffolding protein was able to bind TRPC1 and TRPC4. These observations are in favor of a central role of α1-syntrophin in regulating the sarcolemmal cation channels by a PDZ domain-mediated interaction. This has already been proposed in the case for γ_2-syntrophin for the regulation of SCN5A channels (40).

In the present study, the requirement of α1-syntrophin for regulating cation entry is supported by the effects of repressing α1-syntrophin expression with siRNA. Indeed, α1-syntrophin-deficient myotubes displayed a dysregulation of cation influx similar to that measured in dystrophin-deficient myotubes. These new data suggest that α1-syntrophin plays a central and essential role in mediating the regulation of sarcolemmal cation channels by the DAPC. Moreover, we have shown that the N-terminal part of α1-syntrophin, containing the PDZ domain, is necessary for this regulation. In normal muscle, dystrophin may constitute the scaffold for recruiting α1-syntrophin near the sarcolemmal cationic channels, which constitutes a signaling complex supporting a PDZ-mediated regulation of the cation entry during the activity of muscle cells. We demonstrated previously that TRPC1 channels form a stable molecular complex with native dystrophin and α1-syntrophin in normal muscle (7). Showing the association of TRPC1 with caveolin-3, another component of the DAPC, a recent work from another group (41) confirmed our previous finding (7) in which TRPC channels in skeletal muscle are part of a costameric macromolecular complex. Our new data provide compelling evidence that TRPC4 channels also interact with this macromolecular complex associated with the DAPC. In dystrophic muscles the absence of dystrophin results in a reduction at the sarcolemma of α-syntrophin (3), neuronal nitric-oxide synthase (42, 43), and aquaporin-4 (44). Our results suggest that the drastic decrease in α1-syntrophin at the sarcolemma observed in dystrophin-deficient muscles may participate in the deregulation of slow calcium influx involved in the physiopathology of DMD.

The present study provides evidence that the sarcolemmal cation channels regulated by the α1-syntrophin are constituted at least of TRPC1 and TRPC4 proteins. (i) First, native TRPC4 channels can be coimmunoprecipitated with TRPC1 channels, and both channels are present at the sarcolemma of muscle cells as shown by immunofluorescence. When transfected, recombinant TRPC1 and TRPC4 channels can be expressed at the sarcolemma of differentiated myotubes. (ii) As for TRPC1 channels, TRPC4 could be coimmunoprecipitated with dystrophin and α1-syntrophin or in a recombinant system with mini-dystrophin and Myc-α1-syntrophin. Both TRPC1 and TRPC4 are present in a macromolecular complex associated with the DAPC, and both channels can be fixed *in vitro* by the PDZ domain of α1-syntrophin. (iii) The level of divalent cation influx in myotubes is dependent on the expression of TRPC1 and TRPC4 channels; overexpressing TRPC1 or TRPC4 channels at the sarcolemma increased the cation entry, and conversely, repressing TRPC1 or TRPC4 channels decreased the cation entry, which is in accordance with the observations made previously in sarcolemmal non-voltage-dependent cation currents of muscle fibers (22). This cation entry was sensitive to SKF-96365 but was not affected by nifedipine, a voltage-dependent calcium channel inhibitor. Moreover, the repression of TRPC1 or TRPC4 channels counteracted the increase of cation influx resulting from the knockdown of α1-syntrophin. These observations are clearly in favor of a PDZ domain-mediated regulation by α1-syntrophin of TRPC1- and TRPC4-dependent cation entry through the sarcolemma. TRPC1 can homodimerize through an N-terminal coiled-coil motif (45), but expression studies have indicated that TRPC1 can form heterotetramers with TRPC3, TRPC4, and/or TRPC5 (32, 46, 47). According to other studies, TRPC1 may only form functional channels at the plasma membrane when expressed as heterotetramers, as shown for example in TRPC1/TRPC4 coexpression studies (32, 48). Our coimmunoprecipitation assays are in favor of a heterotetrameric TRPC1/TRPC4 channel interacting with α1-syntrophin and the DAPC. Within the cytosolic region of TRPC channels, several domains could mediate the assembly of macromolecular complexes such as the coiled-coil domain and PDZ-binding motif. This latter motif has already been described for TRPC4 (49, 50), which interacts with a PDZ domain in Na^+/H^+ exchanger regulatory factor. TRPC1 and TRPC4 can be activated in non-excitable cells by the $G_{\alpha q/11}$-linked phospholipase pathway, and both are also shown to form store-operated cationic channels (51, 52). The study of knockout mice has shown that some cell types from $TRPC4^{-/-}$ (53) or $TRPC1^{-/-}$ (11) mice display reduced store-operated calcium entry. Our results obtained with siRNA and overexpression experiments, and the previous study using antisense oligonucleotide in muscle fibers (22), favor of the idea that these sarcolemmal cation channels can be triggered after a store depletion protocol. However, depletion of intracellular calcium stores may not directly activate TRPC-dependent influx, which could be regulated by intracellular calcium and other second messengers that are released after the depletion protocol. Recent studies have shown that SOCEs are mainly dependent on STIM1 and Orai1 in myotubes (54) and that these proteins constitute core components of the SOC. The activity of STIM1 requires an ERM (ezrin/radixin/moesin) domain, which mediates the selective binding of STIM1 to TRPC1 and TRPC4 (15, 55). Interactions among Orai1, TRPCs, and STIM1 (16, 56), as well as the functional requirement for Orai1 in store-operated TRPC1-STIM1 channels (17), raised the question of STIM1 and Orai1 interactions with the sarcolemmal TRPC1 and TRPC4 channels. However, the results obtained with a low concentration of gadolinium (17) suggest that under our experimental conditions TRPC-dependent influx recorded in myotubes is independent of Orai1/STIM1. STIM1 was recently shown to be required for SOCE during sustained activity of skeletal muscles (20). The localization of STIM1 at the membrane of the sarcoplasmic reticulum suggests an interaction at

the T-tubule membrane with SOCs. A complex associating Orai1, TRPC, and STIM1 may thus form store-operated machinery at the triads controlling the calcium influx through the T-tubule membrane (21). It is likely that our quenching assay and partial depletion protocol do not permit recording of this fast entry of cation in the restricted intertriadic space. The sarcolemmal TRPC1/TRPC4 cation channels associated with the costameric DAPC are, however, at another membrane compartment and may be triggered by other mechanisms. Heterologous expression of TRPC1 has provided controversial data concerning the activation of TRPC1-supported currents by stretch (24, 57). In skeletal muscle, however, other studies suggest that TRPC1 also contributes to MS channels in differentiated muscle cells (58) and in C2C12 myoblasts (59). Moreover, stretch-activated currents share similar electrophysiological properties with store-operated currents when recorded at the surface membrane of skeletal fibers (23). Stretch-activated currents (27, 60) and osmotic activated calcium entry (33) are increased in *mdx* and DMD muscle cells lacking dystrophin and DAPC. It is thus possible that the loss of the PDZ-mediated regulation by α1-syntrophin in dystrophin-deficient muscles enhances the mechanical sensitivity of TRPC1-containing channels.

A recent study (41) also proposed that higher levels of TRPC1 and caveolin-3 at the sarcolemma of dystrophin-deficient muscle contribute to abnormal calcium influx as well as to reactive oxygen species and Src kinase activation. A loss of α1-syntrophin combined with higher amounts of TRPC1 and caveolin-3 could thus contribute to altered calcium influx. Interestingly, mice lacking Homer-1, another scaffolding protein, exhibit a myopathy associated with increased spontaneous cation influx dependent on TRPC1 (58). Together, these independent observations show that the regulation of TRPC1 by scaffolding proteins in skeletal muscle is critical for slow non-voltage-dependent calcium entry. Moreover, diminished Homer-1 expression in dystrophic *mdx* mice may also contribute to abnormal cation channel activity in dystrophic myofibers.

Our study reinforces the idea that TRP channels form cation channels, which operate with macromolecular complexes closely associated with the cytoskeleton. Further studies will be necessary to determine the composition of the costameric complex anchored to the dystrophin cytoskeleton and to determine how α1-syntrophin controls the activity of TRPC1 and TRPC4 channels at the sarcolemma.

Acknowledgments—We thank Dr. Craig Montell from The Johns Hopkins University School of Medicine, Baltimore, for giving us the plasmid encoding for TRPC1 and TRPC4 channels. We thank Françoise Mazin for technical assistance.

REFERENCES

1. Ervasti, J. M., and Campbell, K. P. (1991) *Cell* **66,** 1121–1131
2. Peters, M. F., Adams, M. E., and Froehner, S. C. (1997) *J. Cell Biol.* **138,** 81–93
3. Compton, A. G., Cooper, S. T., Hill, P. M., Yang, N., Froehner, S. C., and North, K. N. (2005) *J. Neuropathol. Exp. Neurol.* **64,** 350–361
4. Adams, M. E., Butler, M. H., Dwyer, T. M., Peters, M. F., Murnane, A. A., and Froehner, S. C. (1993) *Neuron* **11,** 531–540
5. Gee, S. H., Madhavan, R., Levinson, S. R., Caldwell, J. H., Sealock, R., and Froehner, S. C. (1998) *J. Neurosci.* **18,** 128–137
6. Connors, N. C., Adams, M. E., Froehner, S. C., and Kofuji, P. (2004) *J. Biol. Chem.* **279,** 28387–28392
7. Vandebrouck, A., Sabourin, J., Rivet, J., Balghi, H., Sebille, S., Kitzis, A., Raymond, G., Cognard, C., Bourmeyster, N., and Constantin, B. (2007) *FASEB J.* **21,** 608–617
8. Yuan, J. P., Kiselyov, K., Shin, D. M., Chen, J., Shcheynikov, N., Kang, S. H., Dehoff, M. H., Schwarz, M. K., Seeburg, P. H., Muallem, S., and Worley, P. F. (2003) *Cell* **114,** 777–789
9. Lockwich, T. P., Liu, X., Singh, B. B., Jadlowiec, J., Weiland, S., and Ambudkar, I. S. (2000) *J. Biol. Chem.* **275,** 11934–11942
10. Ambudkar, I. S. (2007) *Biochem. Soc. Trans.* **35,** 96–100
11. Liu, X., Cheng, K. T., Bandyopadhyay, B. C., Pani, B., Dietrich, A., Paria, B. C., Swaim, W. D., Beech, D., Yildrim, E., Singh, B. B., Birnbaumer, L., and Ambudkar, I. S. (2007) *Proc. Natl. Acad. Sci. U.S.A.* **104,** 17542–17547
12. Varga-Szabo, D., Authi, K. S., Braun, A., Bender, M., Ambily, A., Hassock, S. R., Gudermann, T., Dietrich, A., and Nieswandt, B. (2008) *Pflugers Arch.* **457,** 377–387
13. Feske, S., Gwack, Y., Prakriya, M., Srikanth, S., Puppel, S. H., Tanasa, B., Hogan, P. G., Lewis, R. S., Daly, M., and Rao, A. (2006) *Nature* **441,** 179–185
14. Wu, M. M., Luik, R. M., and Lewis, R. S. (2007) *Cell Calcium* **42,** 163–172
15. Yuan, J. P., Zeng, W., Huang, G. N., Worley, P. F., and Muallem, S. (2007) *Nat. Cell Biol.* **9,** 636–645
16. Liao, Y., Erxleben, C., Abramowitz, J., Flockerzi, V., Zhu, M. X., Armstrong, D. L., and Birnbaumer, L. (2008) *Proc. Natl. Acad. Sci. U.S.A.* **105,** 2895–2900
17. Cheng, K. T., Liu, X., Ong, H. L., and Ambudkar, I. S. (2008) *J. Biol. Chem.* **283,** 12935–12940
18. Kurebayashi, N., and Ogawa, Y. (2001) *J. Physiol.* **533,** 185–199
19. Vig, M., DeHaven, W. I., Bird, G. S., Billingsley, J. M., Wang, H., Rao, P. E., Hutchings, A. B., Jouvin, M. H., Putney, J. W., and Kinet, J. P. (2008) *Nat. Immunol.* **9,** 89–96
20. Stiber, J., Hawkins, A., Zhang, Z. S., Wang, S., Burch, J., Graham, V., Ward, C. C., Seth, M., Finch, E., Malouf, N., Williams, R. S., Eu, J. P., and Rosenberg, P. (2008) *Nat. Cell Biol.* **10,** 688–697
21. Launikonis, B. S., and Rios, E. (2007) *J. Physiol.* **583,** 81–97
22. Vandebrouck, C., Martin, D., Colson-Van Schoor, M., Debaix, H., and Gailly, P. (2002) *J. Cell Biol.* **158,** 1089–1096
23. Ducret, T., Vandebrouck, C., Cao, M. L., Lebacq, J., and Gailly, P. (2006) *J. Physiol.* **575,** 913–924
24. Maroto, R., Raso, A., Wood, T. G., Kurosky, A., Martinac, B., and Hamill, O. P. (2005) *Nat. Cell Biol.* **7,** 179–185
25. Franco-Obregon, A., and Lansman, J. B. (2002) *J. Physiol.* **539,** 391–407
26. Franco-Obregon, A., Jr., and Lansman, J. B. (1994) *J. Physiol.* **481,** 299–309
27. Vandebrouck, C., Duport, G., Cognard, C., and Raymond, G. (2001) *Neuromuscul. Disord.* **11,** 72–79
28. Hopf, F. W., Reddy, P., Hong, J., and Steinhardt, R. A. (1996) *J. Biol. Chem.* **271,** 22358–22367
29. Boittin, F. X., Petermann, O., Hirn, C., Mittaud, P., Dorchies, O. M., Roulet, E., and Ruegg, U. T. (2006) *J. Cell Sci.* **119,** 3733–3742
30. Vandebrouck, A., Ducret, T., Basset, O., Sebille, S., Raymond, G., Ruegg, U., Gailly, P., Cognard, C., and Constantin, B. (2006) *FASEB J.* **20,** 136–138
31. Beech, D. J. (2005) *Pflugers Arch.* **451,** 53–60
32. Hofmann, T., Schaefer, M., Schultz, G., and Gudermann, T. (2002) *Proc. Natl. Acad. Sci. U.S.A.* **99,** 7461–7466
33. Imbert, N., Vandebrouck, C., Constantin, B., Duport, G., Guillou, C., Cognard, C., and Raymond, G. (1996) *Neuromuscul. Disord.* **6,** 351–360
34. Rivet, M., Cognard, C., Rideau, Y., Duport, G., and Raymond, G. (1990) *Cell Calcium* **8,** 507–514
35. Imbert, N., Vandebrouck, C., Duport, G., Raymond, G., Hassoni, A. A., Constantin, B., Cullen, M. J., and Cognard, C. (2001) *J. Physiol.* **534,** 343–355
36. Cognard, C., Lazdunski, M., and Romey, G. (1986) *Proc. Natl. Acad. Sci. U.S.A.* **83,** 517–521
37. Friedrich, O., Both, M., Gillis, J. M., Chamberlain, J. S., and Fink, R. H. (2004) *J. Physiol.* **15,** 251–265

38. Mery, L., Strauss, B., Dufour, J. F., Krause, K. H., and Hoth, M. (2002) *J. Cell Sci.* **115,** 3497–3508
39. Hopf, F. W., Turner, P. R., and Steinhardt, R. A. (2007) *Subcell. Biochem.* **45,** 429–464
40. Ou, Y., Strege, P., Miller, S. M., Makielski, J., Ackerman, M., Gibbons, S. J., and Farrugia, G. (2003) *J. Biol. Chem.* **278,** 1915–1923
41. Gervasio, O. L., Whitehead, N. P., Yeung, E. W., Phillips, W. D., and Allen, D. G. (2008) *J. Cell Sci.* **121,** 2246–2255
42. Brenman, J. E., Chao, D. S., Xia, H., Aldape, K., and Bredt, D. S. (1995) *Cell* **82,** 743–752
43. Chang, W. J., Iannaccone, S. T., Lau, K. S., Masters, B. S., McCabe, T. J., McMillan, K., Padre, R. C., Spencer, M. J., Tidball, J. G., and Stull, J. T. (1996) *Proc. Natl. Acad. Sci. U.S.A.* **93,** 9142–9147
44. Frigeri, A., Nicchia, G. P., Verbavatz, J. M., Valenti, G., and Svelto, M. (1998) *J. Clin. Investig.* **102,** 695–703
45. Engelke, M., Friedrich, O., Budde, P., Schafer, C., Niemann, U., Zitt, C., Jungling, E., Rocks, O., Luckhoff, A., and Frey, J. (2002) *FEBS Lett.* **523,** 193–199
46. Strubing, C., Krapivinsky, G., Krapivinsky, L., and Clapham, D. E. (2001) *Neuron* **29,** 645–655
47. Goel, M., Sinkins, W. G., and Schilling, W. P. (2002) *J. Biol. Chem.* **277,** 48303–48310
48. Alfonso, S., Benito, O., Alicia, S., Angelica, Z., Patricia, G., Diana, K., and Luis, V. (2007) *Cell Calcium* **43,** 375–387
49. Tang, Y., Tang, J., Chen, Z., Trost, C., Flockerzi, V., Li, M., Ramesh, V., and Zhu, M. X. (2000) *J. Biol. Chem.* **275,** 37559–37564
50. Obukhov, A. G., and Nowycky, M. C. (2004) *J. Cell. Physiol.* **201,** 227–23545
51. Zitt, C., Zobel, A., Obukhov, A. G., Harteneck, C., Kalkbrenner, F., Luckhoff, A., and Schultz, G. (1996) *Neuron* **16,** 1189–1196
52. Philipp, S., Cavalie, A., Freichel, M., Wissenbach, U., Zimmer, S., Trost, C., Marquart, A., Murakami, M., and Flockerzi, V. (1996) *EMBO J.* **15,** 6166–6171
53. Freichel, M., Suh, S. H., Pfeifer, A., Schweig, U., Trost, C., Weissgerber, P., Biel, M., Philipp, S., Freise, D., Droogmans, G., Hofmann, F., Flockerzi, V., and Nilius, B. (2001) *Nat. Cell Biol.* **3,** 121–127
54. Lyfenko, A. D., and Dirksen, R. T. (2008) *J. Physiol.* **15,** 4815–4824
55. Huang, G. N., Zeng, W., Kim, J. Y., Yuan, J. P., Han, L., Muallem, S., and Worley, P. F. (2006) *Nat. Cell Biol.* **8,** 1003–1010
56. Liao, Y., Erxleben, C., Yildirim, E., Abramowitz, J., Armstrong, D. L., and Birnbaumer, L. (2007) *Proc. Natl. Acad. Sci. U.S.A.* **104,** 4682–4687
57. Gottlieb, P., Folgering, J., Maroto, R., Raso, A., Wood, T. G., Kurosky, A., Bowman, C., Bichet, D., Patel, A., Sachs, F., Martinac, B., Hamill, O. P., and Honoré, E. (2008) *Pflugers Arch.* **455,** 1097–1103
58. Stiber, J. A., Zhang, Z. S., Burch, J., Eu, J. P., Zhang, S., Truskey, G. A., Seth, M., Yamaguchi, N., Meissner, G., Shah, R., Worley, P. F., Williams, R. S., and Rosenberg, P. B. (2008) *Mol. Cell. Biol.* **28,** 2637–2647
59. Formigli, L., Francini, F., Nistri, S., Margheri, M., Luciani, G., Naro, F., Silvertown, J. D., Orlandini, S. Z., Meacci, E., and Bani, D. (2009) *J. Mol. Cell. Cardiol.* **47,** 335–345
60. Franco, A., Jr., and Lansman, J. B. (1990) *J. Physiol.* **427,** 361–380